CHAPTER 6

EFFECT OF ULTRASONIC SHOT PEENING ON CORROSION RESISTANCE, BIOCOMPATIBILITY, FATIGUE AND CORROSION FATIGUE BEHAVIOR OF THE INDIGENOUSLY DEVELOPED NICKEL-FREE AUSTENITIC STAINLESS STEEL (HNS-Mo)

6.1. Introduction

This chapter presents the influence of USP on electrochemical corrosion in simulated body fluid (SBF), *in vitro* cell culture and proliferation, high cycle fatigue and corrosion fatigue of the HNS-Mo. An effort was made to get an optimized condition of USP for the overall global properties and lifetime enhancement of the HNS-Mo. Samples were prepared and were USPed for different durations of 0.5, 1 and 2 minutes, using 2 mm and 3 mm diameter shots and these are designated as USP 2-0.5, USP 2-1, USP 2-2, USP 3-0.5, USP 3-1 and USP 3-2, respectively. The potentiodynamic polarization, *in vitro* cell culture and proliferation experiments, were conducted following the USP of the HNS-Mo to observe the effect of USP. High cycle fatigue behavior is also studied in air at 30 Hz frequency, following USP, and the results are compared with that of the non-treated (Un-USP) samples. Corrosion fatigue behavior of the HNS-Mo, following USP, is studied at 5 Hz frequency, and it is compared with that of the Un-USP. USP for 3 minutes with 3 mm shots was given in the gauge section of the fatigue samples for high cycle fatigue testing in air and SBF and they are designated as USP 3-3. Enhancement in breakdown potential and cell proliferation is observed, following USP. High cycle fatigue life and endurance limit, following USP, are found to increase significantly and it is discussed in terms of delay in crack initiation caused by the inducement of compressive residual stress, enhancement in strength and microstructural modification

due to USP. The corrosion fatigue endurance limit corresponding to 10^7 cycles increases significantly, following USP, due to synergistic improvement in corrosion resistance and fatigue life.

6.2. Effect of Ultrasonic Shot Peening on Corrosion Behavior of the HNS-Mo

The HNS-Mo was characterized for its electrochemical corrosion behavior, following USP in various conditions. The potentiodynamic polarization curves are presented in **Fig. 6.1**.

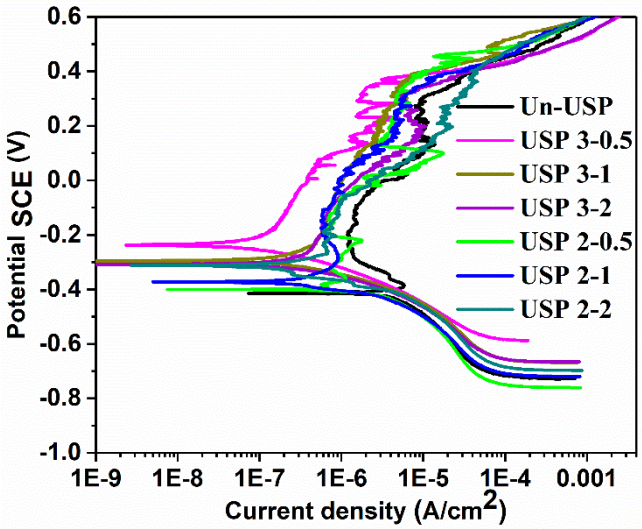

Fig. 6.1. Potentiodynamic polarization plots of the HNS-Mo in various USPed conditions.

The different corrosion parameters are analyzed and are given in **Table 6.1**. Corrosion potential (E_{corr}) values of the USPed samples are more positive, i.e., noble, than that of the Un-USP sample. The E_{corr} value is found highest (-238 mV_{SCE}) for the USP 3-0.5 condition. There is decrease in the E_{corr} with the duration of USP for the 3 mm shots; whereas, an increase is observed with USP duration in the specimens treated with 2 mm shots. Also, the samples USPed with 3 mm shots show nobler behavior than those USPed with 2 mm shots. It can be seen from **Fig. 6.1** and Table **6.1** that there is an increase in the breakdown potential following USP. The breakdown potential increased for the USP

3-0.5 and USP 3-1 as compared to the Un-USP, whereas there is drastic decrease in the breakdown potential for the USP 3-2 compared to the USP 3-1 but it is comparable to that of the Un-USP. Breakdown potential for the USP 2-0.5, USP 2-1 and USP 2-2 is higher than that of the Un-USP. Interestingly, there is no drastic decrease in the breakdown potential for the USP 2-2, which is observed for the USP 3-2.

Table 6.1. Corrosion data of HNS-Mo in various conditions.

Material	**Corrosion potential, E_{corr} (mV_{SCE})**	**Breakdown potential, E_{bd} (mV_{SCE})**	**Critical current density, i_{cr} ($\mu A/cm^2$)**	**Current density at 200 mV, i_p ($\mu A/cm^2$)**
HNS-Mo (UN-USP)	-413	310	5.78	10.3
USP 3-0.5	-238	370	0.12	2.5
USP 3-1	-295	387	0.47	3.1
USP 3-2	-309	308	0.37	8.4
USP 2-0.5	-399	395	0.67	4.1
USP 2-1	-373	375	0.90	4.8
USP 2-2	-311	398	0.68	17.4

Critical current density (i_{cr}) was also evaluated from the potentiodynamic plots. It can be seen from **Table 6.1** that there is significant decrease in i_{cr} of the USPed samples as compared to that of the Un-USP. The current density measured in the passive region at 200 mV_{SCE} shows similar trend, except for the USP 2-2 condition. Overall, USP 3-0.5 sample exhibits the best result.

6.3. Effect of Ultrasonic Shot Peening on Cell culture and Proliferation of the HNS-Mo

The effect of USP on MG-63 cell culture on HNS-Mo is shown in **Fig. 6.2**.

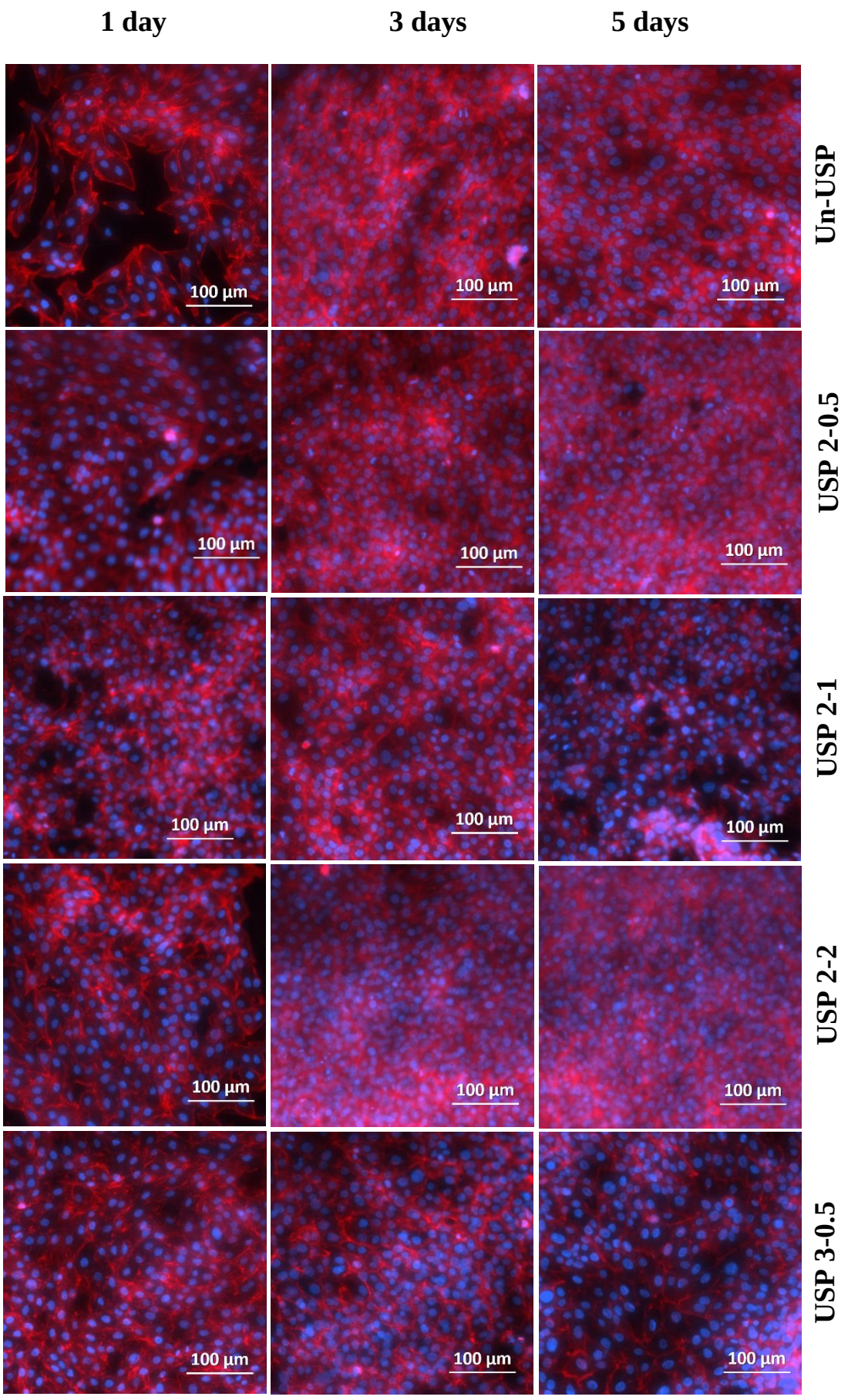
1 day
3 days
5 days
Un-USP
USP 2-0.5
USP 2-1
USP 2-2
USP 3-0.5
100 µm

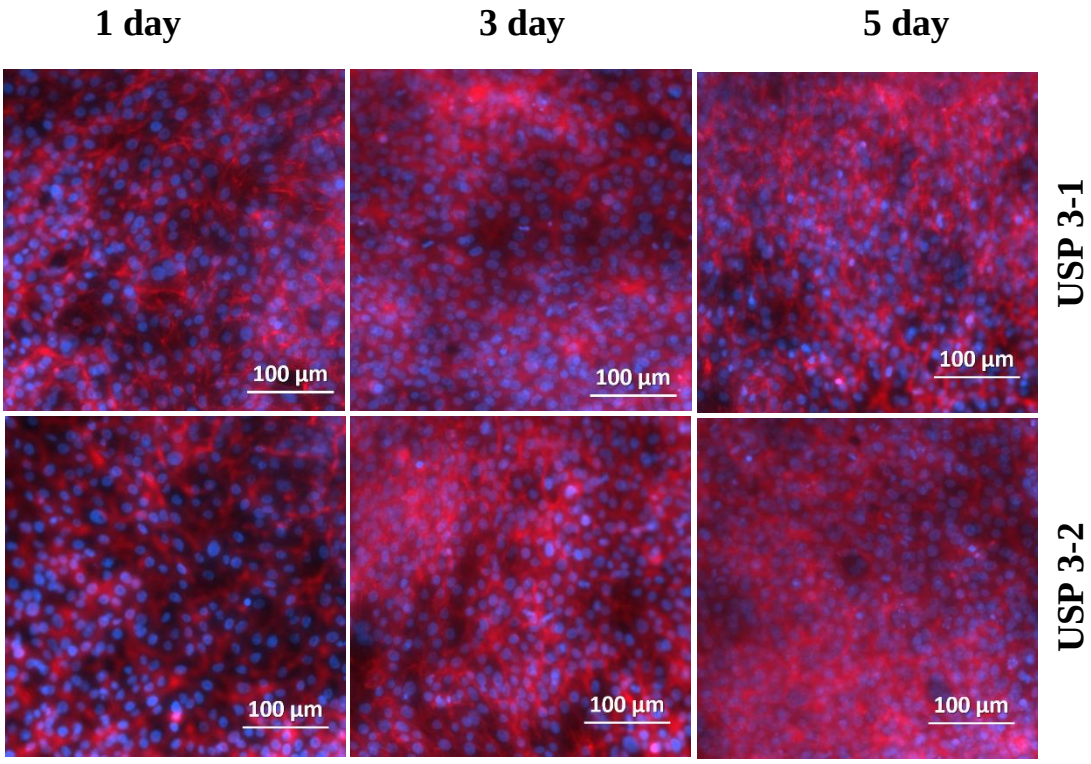

Fig. 6.2. Panel representing the fluorescent cell culture images of MG-63 human bone osteosarcoma cells on the HNS-Mo samples in various USPed conditions; after 1 day, 3 days and 5 days of incubation. Blue color: nuclei staining; red color: actin cytoskeleton filament staining.

There is increase in cell coverage with increase in the duration of incubation for all the samples, which shows that there is no inhibition in cell growth and spreading, following USP. Distinct higher cell coverage can be seen clearly on the USPed samples than on the Un-USP, indicating a more increased cell proliferation over the USPed samples than the Un-USP.

The cell proliferation behavior of the MG-63 cells in the different USPed conditions was studied by MTT assay and is shown in **Fig. 6.3**. It is clear from the histograms that there is a gradual increase in cell proliferation with the duration of incubation for all the conditions. The proliferation of the MG-63 cells on the USPed samples is found to increase significantly with the duration of incubation. The statistical analysis shows that the difference in the levels of cell proliferation for the different time points is significant

at the level of 0.05. For the USP 3-2 condition, there is increase in the mean percentage cell proliferation compared to the Un-USP condition. A significant difference between the various groups is observed only for the USP 3-1 and USP 3-2 conditions with respect to the Un-USP after 5 days of incubation**.**

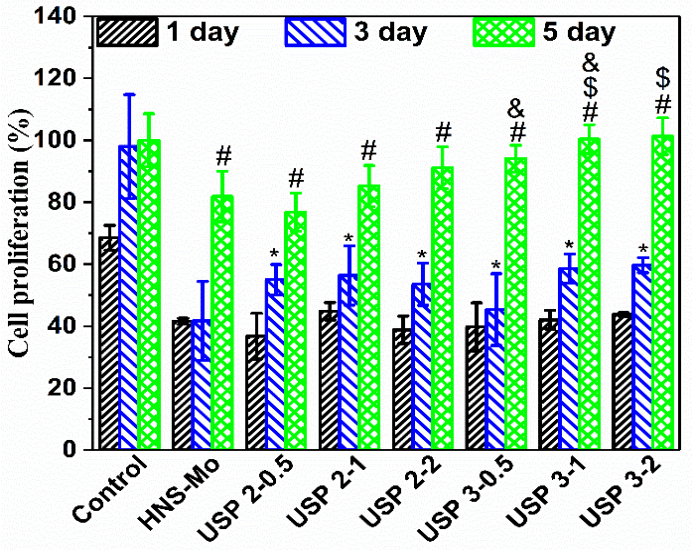

Fig. 6.3. Histograms representing comparison of MG-63 cell proliferation after 1, 3 and 5 days of incubation by MTT assay for the HNS-Mo in various USPed conditions. In this experiment, absorbance of control for the 5th day culture was taken as reference for all the samples. $^{*}p \leq 0.05$ with respect to 1 day of corresponding group. $^{\#}p \leq 0.05$ with respect to 3 days of corresponding group. $^{\$}p \leq 0.05$ with respect to Un-USP for the same day. $^{\&}p \leq 0.05$ with respect to USP 2-1 for the same day.

6.4. Effect of Ultrasonic Shot Peening on High Cycle Fatigue and Corrosion Fatigue of the HNS-Mo

High cycle fatigue life is one of the essential requirements of biomedical materials. It is susceptible to the surface condition of materials. There was improvement in corrosion resistance of the HNS-Mo, following USP, and also enhancement in cell proliferation was observed up to a certain limit. Therefore, the effect of USP on the high cycle fatigue performance of the HNS-Mo in air and simulated body fluid (SBF) environment is

studied. The fatigue life endured by the HNS-Mo in Un-USP and USP 3-3 conditions, tested at different stress levels is shown in **Table 6.2**.

Table: 6.2. Comparison of high cycle fatigue life of the HNS-Mo austenitic stainless steel for the USP 3-3 and Un-USP conditions, at various maximum stresses in air and SBF environment.

Maximum stress, MPa	**Fatigue life (N_f)**			
	In air		**In SBF**	
	Un-USP	**USP 3-3**	**Un-USP**	**USP 3-3**
610	-	442779	-	-
600	-	586668	-	-
590	298377	1252240	-	-
	274646			
572	505170	NF	273673	NF
	471045		447361	
560	-	NF	-	NF
550	759624		615223	-
			628543	
538	1136100		1303120	-
	1188830		1408250	
525	7389220		1984250	-
	NF		2045300	
513	NF		3443620	-
500	NF		8721000	-
475			NF	-

Note: NF: not failed at 10^7 cycles

The dependence of number of cycles (log N) on the stress for the HNS-Mo in the Un-USP and USPed condition is shown in **Fig. 6.4**. A significant improvement in fatigue life may be observed following the USP for 3 minutes with 3 mm shots. The stress at which samples did not fail after 10^7 cycles, was considered as endurance limit. The endurance limit of the HNS-Mo increased from 513 MPa to 572 MPa, following USP, in air, which

is shown by solid arrows **(Fig. 6.4a)**. At the maximum stress of 590 MPa, there is more than three times increase in fatigue life, following USP. More importantly, the corrosion fatigue life of the HNS-Mo increased significantly for the USP 3-3 samples compared to the Un-USP. The endurance limit has increased up to 572 MPa from 475 MPa for the USP 3-3 condition **(Fig. 6.4b)**.

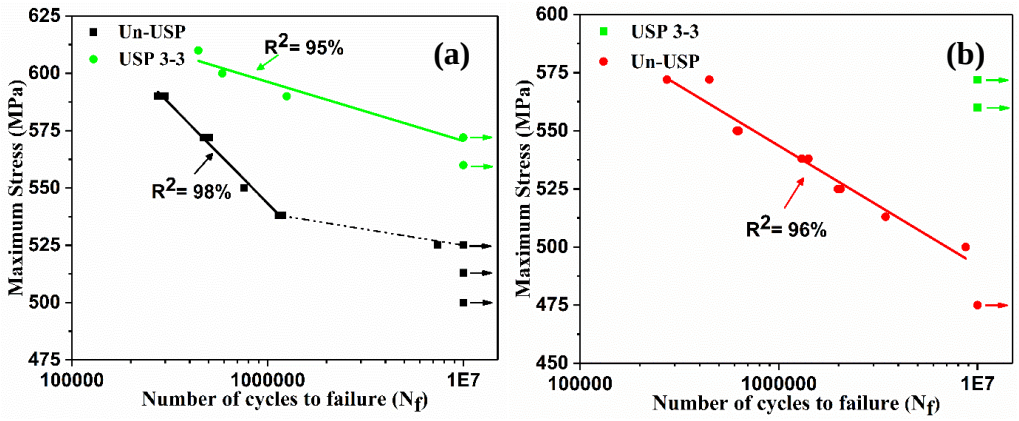

Fig. 6.4. Comparison of high cycle fatigue life of the HNS-Mo in the Un-USP and USP 3-3 conditions in (a) air, and (b) SBF.

Thus, it can be seen that the USP can eliminate the negative effect of SBF environment on fatigue strength. To evaluate the effect of USP on endurance limit of the HNS-Mo, the increment rate of endurance limit (IREL) is used and is determined as shown in **Eq. 6.1**.

$$\text{IREL} = \frac{\sigma_{USP} - \sigma_{Un-USP}}{\sigma_{Un-USP}} \quad (6.1)$$

The IREL for the HNS-Mo in air and in SBF are 11.50 % and 20.42 %, respectively.

6.5. Discussion

6.5.1. Effect of Ultrasonic Shot Peening on Corrosion Behavior

USP significantly affects the surface condition of the material, which can influence its corrosion resistance. There is refinement of the coarse-grained microstructure to nanoscale, inducement of compressive residual stress, increase in defect density/surface

defects and microstrain, increase in surface roughness, following USP, which in turn altogether affect the corrosion resistance of stainless steels. In addition to that corrosion behavior of stainless steel depends on the corrosive medium, solubility/stability of corrosion products in corrosive medium and ability to form a passive film on the surface. Chloride (Cl^-) ions are present in the SBF solution and HNS-Mo readily forms a passive film on the surface and breaks after attaining specific potential, as shown in the previous chapter. The passive oxide film of CrMnMoN based stainless steels consists of iron oxide and chromium oxide, where iron oxide is in the outer layer and chromium oxide is in inner layer of the passive oxide film [87].

Improvement in breakdown potential (E_{bd}) of the HNS-Mo was observed following USP, irrespective of the duration and size of shots used for the USP. There is severe plastic deformation in surface region of the material following USP. An enhancement in corrosion resistance of the CrMnMoN based alloys was observed following cold working, which was attributed to increase in resistance of the passive film formed [206]. Shallower and smaller pits were observed in the cold-worked stainless steel. However, breakdown potential was found to increase significantly due to nanostructuring. It enhances the passivation, which is attributed to enrichment of Cr at the surface [156]. An increase in passive current density was observed for the nanocrystalline nickel due to the defective nature of the passive film [155]. Nanocrystallisation caused by USP has a significantly high number of grain boundaries and uniformity in the elemental distribution. The grain boundary is a high-energy region that could provide a high density of nucleation sites. Initially, there will be a rapid dissolution of elements which may lead to formation and presence of very high amount of NH_4^+ to promote repassivation and inhibit the growth of pits [67]. An increase in the uniformity in the distribution of Cr in the passive film of nanostructured material has been reported for the 309 steel [156].

Therefore, a nanostructured surface with a highly uniform distribution of elements can promote rapid formation of Cr rich highly protective passive oxide layer on the surface compared to the Un-USP specimen. Interaction of Cl^- containing corrosive media with surface promotes rapid corrosion and there is enrichment in Cr and N content on the surface due to selective leaching of other elements. Consequently, there is an increase in pitting resistance of the HNS-Mo following USP.

Apart from the grain size at the surface, there are many others factors like residual stress, surface roughness, phase transformation, surface defects, etc., which influence the corrosion resistance of stainless steels [194]. Compressive residual stress decreases the current density [195]. USP is found to induce compressive residual stress in stainless steel. The significant decrease in the current density is associated with the inducement of compressive residual stress. The samples USPed with 3 mm shots show better corrosion resistance than those USPed with 2 mm shots. This disparity in the result may be due to the higher compressive residual stress associated with the samples, USPed with 3 mm shots. An increase in the critical current density of the specimen, treated with 3 mm shots, with increase in the USP duration is observed (**Table 6.1**). It may be due to the comparatively non-uniform nature of the passive film. Since the 3 mm diameter shots have comparatively more kinetic energy, a longer duration of USP causes erosion of the surface, producing inhomogeneity in the surface and, consequently, in the passive film. There is an increase in the critical current density.

6.5.2. Effect of Ultrasonic Shot Peening on Cell Culture and Proliferation

The cell adhesion and proliferation depend on the physicochemical condition of the surface of stainless steel [131]. The presence of higher number of grain boundaries and nanocrystalline microstructure at the surface promotes the cell adhesion and proliferation by increasing the protein adsorption at the surface [198]. The surface topography and

nanostructured surface increase the wettability which in turn enhances the cell response [199]. The induced compressive stress in the surface region, following USP, is found to change the distribution without changing the morphology of cells and decrease in cell density was observed in the high compressive stress region [200]. Therefore, grain refinement and surface morphology increase the cell activity, whereas the compressive stress in the surface region restricts the activity of cells.

There is gradual increase in the cell coverage and mean percentage cell proliferation with the duration of incubation for all the Un-USP and USPed conditions. It shows that there was no inhibition of cell activity, following the USP. MG-63 cells have either increased cell activity with USP or have no effect. There is decrease in grain size with increase in USP duration. However, there is increase in residual stress with increase in the duration of USP and shot diameter. Therefore, the difference in the effectiveness of the beneficial role of grain refinement and the detrimental role of the compressive stress, determines the cell response following USP.

Additionally, leaching out of different elements significantly influences cell activity. There is an improvement in corrosion resistance, following USP, which will reduce the release rate of ions and the presence of ions that can affect the cell activity in long-term implantation. Also, the chances of contamination in the implanted region will reduce during the long-term implantation due to increased corrosion resistance and the reliability of implants will increase.

6.5.3. Effect of Ultrasonic Shot Peening on High Cycle Fatigue and Corrosion Fatigue Life

The influence of USP on the high cycle fatigue and corrosion fatigue was studied following 3 minutes of USP with 3 mm shots. The corrosion resistance and biocompatibility are found to increase for the shorter duration of USP and for longer

duration of USP, there is deterioration in corrosion resistance. Also, the bigger size of shots induces comparatively higher residual stress and the depth of gradient structure. Disc type of samples were used for the corrosion and biocompatibility testing, and cylindrical specimens were used for fatigue testing. The microstructural modification observed up to the depth of ~ 100 µm after 30 seconds of USP for the disc type of samples was equivalent to those of 3 minutes USPed cylindrical fatigue samples. Therefore, USP 3-3 condition was selected for the high cycle fatigue testing considering all these factors. High cycle fatigue is a surface sensitive phenomenon. The number of cycles endured before failure consists of cycles for crack initiation and crack propagation, and these depend on surface microstructure, residual stress on the surface, material strength, and related stress at which tests are conducted. USP causes surface grain refinement to nanoscale, induces compressive residual stress, increases surface roughness. Following USP, a gradient microstructure is generated in which there is nanostructure at the surface and from surface to interior there is gradual increase in the grain size which significantly improves the strength of the material [144]. During USP, there is severe plastic deformation of material due to very high strain and strain rate. High nitrogen-containing stainless steels are found to deform via mechanical twinning at higher strain [207]. There is extensive intersection of twins due to USP. Twin intersection increases the strength of high nitrogen-containing stainless steel significantly [208]. Zhang et al. [209] found a significant improvement in yield strength of a high nitrogen stainless steel, following friction stir processing, in which a complex structure consisting of ultrafine grain surface and coarse grain base material was developed. It is well known that nanostructured materials have higher strength than coarse-grained materials; likewise, there was significant improvement in the strength of the HNS-Mo, following USP due to nanostructured surface and intersections of twins in interior. Material with higher strength causes less fatigue damage for the same stress amplitude [184]. Therefore,

higher strength material inhibits the early initiation of slip band compared to the lower strength material, which hinders the early crack initiation and fatigue failure.

Fatigue cracks generally initiate from the surface defects generated during cyclic deformation. It is well known that cracks usually initiate from the intrusion/extrusion and slip bands formed at the surface due to repeated loading. However, high cycle fatigue cracks preferentially initiated along the annealing twin of high manganese and nitrogen-containing stainless steel [100]. The nanostructured surface layer reduces the possibility of twin boundaries on the surface and hinders the formation of slip bands due to the relatively uniform and small size of grains. Therefore, surface nanostructuring impedes the crack initiation due to the presence of large number of uniform grain boundaries which reduces the dislocation gliding and slip band formation at the surface [158]. It is well known that compressive residual stress, induced during the USP, suppresses the crack initiation and propagation [203]. Overall, surface nanostructure, inducement of compressive residual stress, and enhanced strength due to extensive intersections of twins and nanostructured surface, suppress the crack initiation, and gradient structure favors the inhibition of crack propagation, and there is enhancement in fatigue life of the HNS-Mo, following USP.

The fatigue behavior of stainless steel in simulated body fluid (SBF) environment is different from that in air. There is continuous interaction of material with the environment and fatigue life is decreased due to the synergistic effect of dynamic loading and corrosion, called corrosion fatigue. The passive film formed on the surface of the stainless steel gets broken during dynamic loading and a fresh surface comes into contact of the environment. In the present study, there is 20.42 % increase in the endurance limit of the USPed sample compared to that of the Un-USP, in SBF environment. This increase in the corrosion fatigue resistance, following USP, may be essentially due to the delay in the process of fatigue crack initiation.

6.6. Conclusions

The effect of USP on corrosion behavior, cell proliferation, high cycle fatigue and corrosion fatigue of the HNS-Mo was evaluated for the orthopedic implant application. There is improvement in pitting corrosion resistance of the USPed samples of the HNS-Mo with respect to the Un-USP condition. However, longer duration of USP decreases the corrosion resistance as compared to the shorter duration. The best result is obtained for the USP 3-0.5 condition. The cell culture and proliferation behavior of the MG-63 cells for 1 day, 3 days and 5 days of incubation are evaluated. The cell coverage increased with the duration of incubation for both, Un-USP and USPed conditions, and higher coverage of attached cells was observed for the USPed samples. The mean percent cell proliferation was also evaluated, following USP; there is no significant improvement in the cell proliferation following the USP after incubation of 1 day, irrespective of the USP condition. Significant improvement in cell proliferation is observed for the USP 3-1 and USP 3-2 samples compared to the Un-USP after 5 days of incubation for the MG-63 cells. The high cycle fatigue life of the HNS-Mo is improved significantly following USP with 3 mm shots for 3 minutes of duration. The endurance limit is increased from 513 MPa to 572 MPa in air and 475 MPa to 572 MPa in simulated body fluid environment.

Improvement in corrosion resistance, biocompatibility and fatigue life has been observed following USP for the HNS-Mo. Improved corrosion resistance will reduce the chances of contamination in the region of implant during long-term implantation. Higher cell activity will increase cell compatibility and reduce inflammation and other related problems. The increased fatigue life and endurance limit will increase the life of the implant. Overall, the USP of the HNS-Mo will increase the reliability of the implants made of nickel free high nitrogen containing stainless steel.